Energetics of Small Clusters of Stabilized Jellium: Continuum and Shell-Structure Effects

MARTA BRAJCZEWSKA and CARLOS FIOLHAIS
Departamento de Física da Universidade de Coimbra, P-3000 Coimbra, Portugal

JOHN P. PERDEW
Department of Physics and Quantum Theory Group, Tulane University, New Orleans, Louisiana, 70118

Abstract

We evaluate binding energies, ionization energies, and second-order energy differences as functions of valence electron number for small spherical clusters of stabilized jellium, using the Kohn–Sham equations with the local-spin-density (LSD) approximation. Cohesive energies are also reported. A comparison is made with semiclassical formulas (liquid drop model and Padé approximant, with surface and curvature coefficients derived from first principles). These formulas nicely average the shell-structure oscillations of the energy, which are found to be almost the same as for ordinary jellium. Spherical clusters with 1, 7, and 9 electrons have binding energies very close to those of the semiclassical predictions.

Introduction

In the simple metals, the delocalized valence electrons experience a weak ionic pseudopotential, which in simplified treatments is often replaced by the potential of a uniform positive background with a sharp boundary (jellium).

The stabilized jellium model [1] for surface and cohesive properties of simple metals is intended to cure well-known deficiencies of the ordinary jellium model: unrealistic results for the binding energies at all densities, for the compression properties at low densities (negative bulk modulus for the density of cesium), and for the surface properties at high densities (negative surface tension for the density of aluminum). All these unrealistic results follow from the fact that jellium is unstable, except at a density close to that of sodium. At that density, jellium and stabilized jellium have identical surface properties. The stabilized jellium model retains the simplicity and universality of jellium. With only two inputs, the density and valence, this model provides an accurate overall description of the binding energies of all simple metals, in the framework of density-functional methods. Given only the density, it delivers reasonable overall surface properties (work function, surface tension, etc.). This result is achieved by subtracting from the energy functional of the jellium model the spurious self-interaction of the bulk positive charge and by introducing inside the solid a constant potential, the average value in the Wigner—

International Journal of Quantum Chemistry: Quantum Chemistry Symposium 27, 249–261 (1993)
 CCC 0020-7608/93/010249-13

TABLE I. Liquid drop model coefficients a_v, a_s and a_c. The surface and curvature coefficients are from a Kohn–Sham calculation for the planar surface of stabilized jellium [8]. Also indicated are the work function W and the distance x_0 from the image plane to the jellium edge of the planar surface, from [9].

	r_s (bohr)	a_v (eV)	a_s (eV)	a_c (eV)	W (eV)	x_0 (bohr)
Al	2.07	−10.58	0.87	0.65	4.27	1.01
Na	3.99	−6.26	0.59	0.24	2.94	1.27
Cs	5.63	−4.64	0.42	0.13	2.26	1.55

Seitz cell of the difference between a local pseudopotential and the jellium background potential.

The jellium model should have the same drawbacks for metallic clusters as for the bulk system. For example, it does not yield realistic binding energies, and it is completely inadequate to describe compression effects of finite systems. Notwithstanding these deficiencies, the jellium model with the help of density-functional methods has been extensively used for understanding metallic clusters [2,3,4]. Those studies support the image of the cluster as a system of electrons bound in a one-particle potential due to the spherical (or deformed) jellium background and the other electrons. Clusters with "magic" numbers of electrons (2, 8, 18, 20, etc.) are more stable than their neighbors, due to the presence of larger gaps above the highest occupied level. The occurrence of ionization energies with local maxima for magic systems corroborates that picture.

Here we shall evaluate the effect of the "stabilization" of jellium on static properties of clusters, such as binding energies, ionization energies and second-order energy differences. In other work [5], the stabilized jellium model will be applied to describe compression effects for clusters at any density.

This work calculates energies of small spherical stabilized jellium clusters, as functions of electron number, using the Kohn–Sham equations of density-functional theory (within the local-spin-density approximation, LSD). By "small," we mean that the number of valence electrons is $N \leq 20$. The quantal energy of the cluster is compared with a classical liquid drop formula. A variant of the liquid drop formula, using a Padé approximant, which has been proposed recently for the study

TABLE II. Padé coefficients for the stabilized jellium model [5]. The r_s values are those of Table I.

	b_1	b_2	b_3
Al	0.742	0.326	0.123
Na	0.399	0.284	0.146
Cs	0.308	0.227	0.147

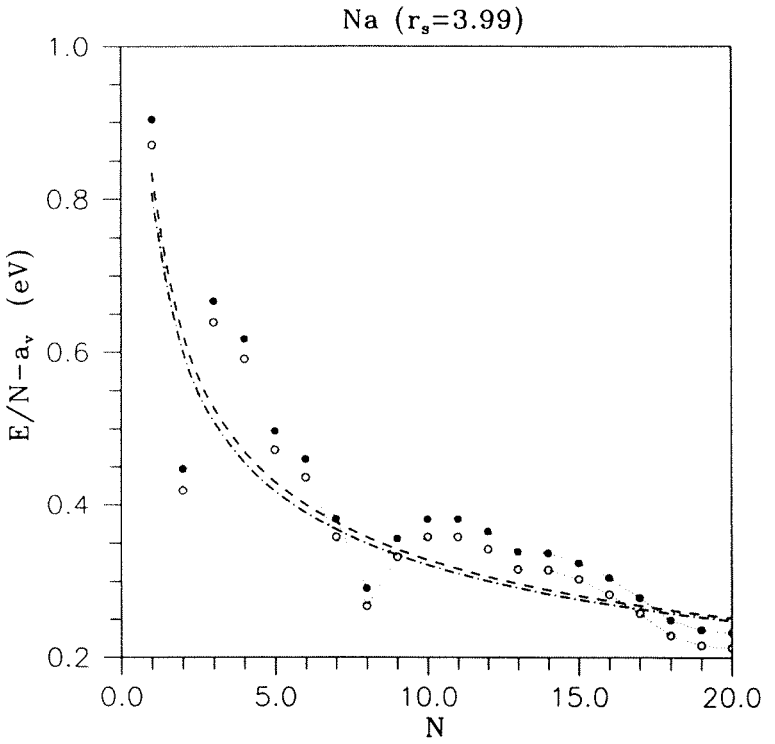

Figure 1. Non-bulk binding energy per valence electron $E/N - a_v$ for clusters of sodium ($r_s = 3.99$), within the stabilized jellium model. The symbols ● and ○ represent, respectively, the Kohn–Sham results for stabilized and ordinary jellium. The dashed line represents the liquid drop model, and the dashed-dotted line the Padé approximant. The bulk binding energy is $a_v = -6.26$ eV for stabilized jellium and $a_v = -2.10$ eV for jellium.

of small voids inside solids [6], is also considered. The enhancement of stability due to shell effects, which is known for jellium, is examined for stabilized jellium. Ionization energies of stabilized jellium clusters are evaluated. Finally, the energies of stabilized jellium atoms are used together with bulk binding energies to obtain cohesive energies.

In the next section, we present the Kohn–Sham equations applied to spherical clusters of stabilized jellium. Results are then displayed for the energetics of three metals (Al, Na and Cs), which cover the whole range of metallic densities. In the last section, further work with stabilized jellium is proposed.

Kohn–Sham Equations for a Cluster of Stabilized Jellium

Let us adopt the atomic system of units ($e = m = \hbar = 1$). We consider a spherical uniform positive background of finite density n_+ such that

$$n_+(\mathbf{r}) = \bar{n}\,\Theta(R - r), \qquad \Theta(R - r) = \begin{cases} 1 & (r \leq R) \\ 0 & (r \geq R)\,, \end{cases} \tag{2.1}$$

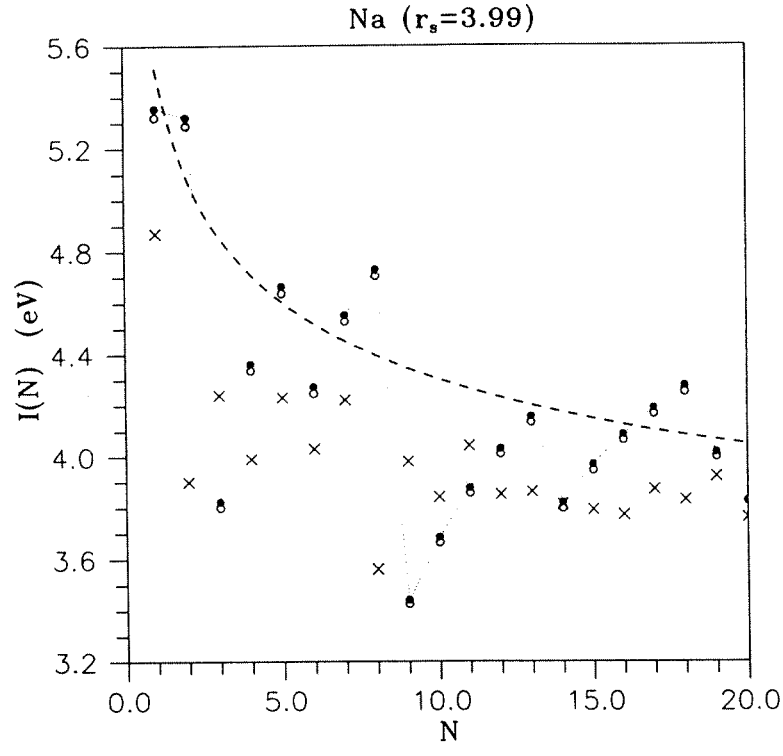

Figure 2. Ionization energies for clusters of sodium. The symbols ● and ○ represent, respectively, stabilized and ordinary jellium results. The dashed line represents the result of formula (2.22) for the stabilized jellium model. Experimental data are indicated by X [22].

with

$$\bar{n} = \frac{3}{4\pi r_s^3} = \frac{k_F^3}{3\pi^2}, \tag{2.2}$$

and R the cluster radius. From the neutrality condition

$$\int d^3r\, n_+(\mathbf{r}) = N, \tag{2.3}$$

the radius of the background sphere must be

$$R = N^{1/3} r_s. \tag{2.4}$$

The self-consistent Kohn–Sham equation is

$$[-\tfrac{1}{2}\nabla^2 + v_{\text{eff}}(\mathbf{r}, \sigma)]\psi_{\alpha\sigma}(\mathbf{r}) = \varepsilon_{\alpha\sigma}\psi_{\alpha\sigma}(\mathbf{r}), \tag{2.5}$$

where α denotes a set of quantum numbers and σ is a spin number (up $\uparrow$ or down $\downarrow$).

In Eq. (2.5), the effective potential is

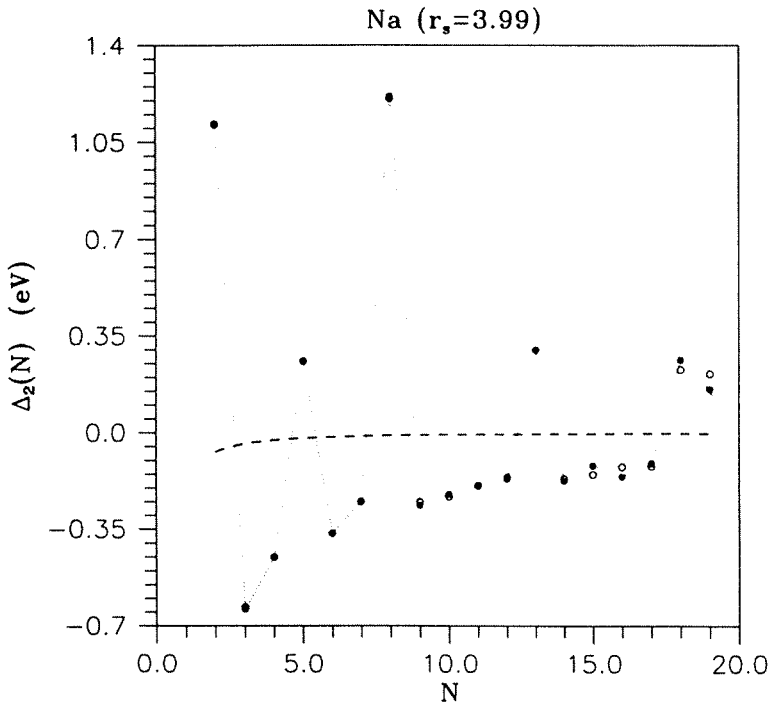

Figure 3. Second-order energy differences for clusters of sodium. The symbols ● and ○ represent, respectively, stabilized and ordinary jellium results. The dashed line represents the liquid drop model for stabilized jellium.

$$v_{\text{eff}}(\mathbf{r}, \sigma) = v_+(\mathbf{r}) + \int d^3r' \frac{n(\mathbf{r}')}{|\mathbf{r} - \mathbf{r}'|} + \mu_{xc}^{\sigma}(\mathbf{r}), \tag{2.6}$$

where v_+ is the electrostatic potential for the interaction between the background and the electrons, $n(\mathbf{r})$ is the total electronic density, and $\mu_{xc}^{\sigma}(\mathbf{r})$ the spin-dependent exchange-correlation potential. We have

$$v_+(\mathbf{r}) = \begin{cases} -\dfrac{N}{2R}\left[3 - \left(\dfrac{r}{R}\right)^2\right] + \langle \delta v \rangle_{\text{WS}} & (r < R) \\ -\dfrac{N}{r} & (r > R), \end{cases} \tag{2.7}$$

with

$$\langle \delta v \rangle_{\text{WS}} = -\frac{k_F^2}{5} + \frac{k_F}{4\pi} + \frac{r_s}{3}\frac{d\varepsilon_c}{dr_s}, \tag{2.8}$$

the average potential difference which appears in the stabilized jellium model [1]. (ε_c is the correlation energy per electron of the uniform electron gas [7].) The second term in (2.6) is the Hartree potential. The last term is the exchange-correlation potential

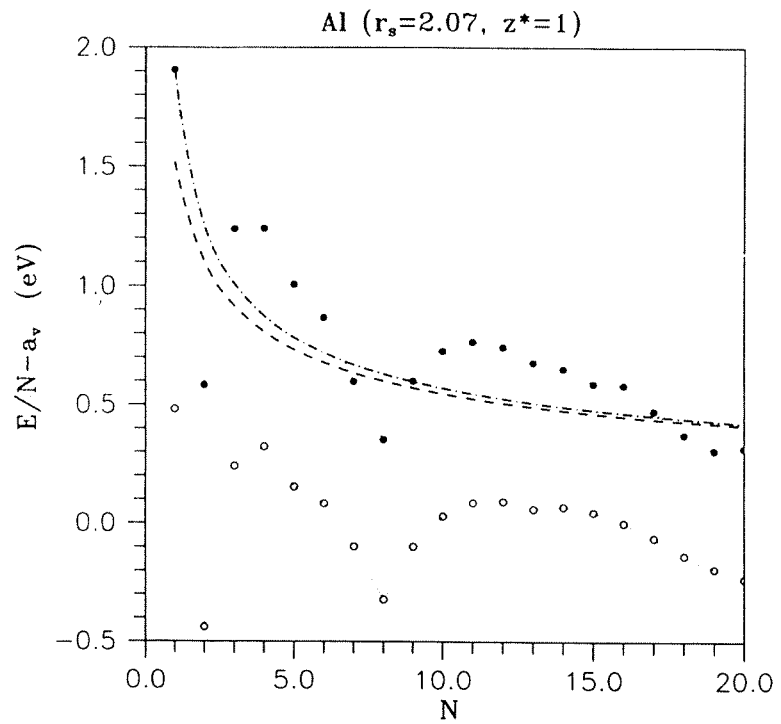

Figure 4. The same as Figure 1 for aluminum ($r_s = 2.07$). The bulk binding energy is $a_v = -10.59$ eV for stabilized jellium and $a_v = -0.21$ eV for jellium.

$$\mu_{xc}^{\sigma}(n_\uparrow(\mathbf{r}), n_\downarrow(\mathbf{r})) = \frac{\partial}{\partial n_\sigma}[n\varepsilon_{xc}(n_\uparrow, n_\downarrow)], \tag{2.9}$$

where $n_\uparrow(\mathbf{r})$ and $n_\downarrow(\mathbf{r})$ are the up and down spin densities, respectively. Here $\varepsilon_{xc} = \varepsilon_x + \varepsilon_c$, with $\varepsilon_x = -3k_F/4\pi$ the exchange energy per electron of the uniform gas.

The total electronic density is given by

$$n(\mathbf{r}) = \sum_{\sigma=\uparrow,\downarrow} n_\sigma(\mathbf{r}), \tag{2.10}$$

with

$$n_\sigma(\mathbf{r}) = \sum_{\alpha} f_{\alpha\sigma}|\psi_{\alpha\sigma}(\mathbf{r})|^2 . \tag{2.11}$$

The $f_{\alpha\sigma}$ are occupation numbers of the orbitals defined by the quantum numbers $\alpha\sigma$ ($f_{\alpha\sigma} = \Theta(\varepsilon_F - \varepsilon_{\alpha\sigma})$, with ε_F the Fermi energy, and $\sum_{\alpha\sigma} f_{\alpha\sigma} = N$).

The total energy of the stabilized jellium cluster is

$$E(N) = \sum_{\alpha\sigma} f_{\alpha\sigma}\varepsilon_{\alpha\sigma} - \left(U[n] + \sum_{\sigma}\int d^3r\, \mu_{xc}^{\sigma}(n_\uparrow, n_\downarrow)n_\sigma(\mathbf{r})\right) + U_B[n_+] + \int d^3r\, \varepsilon_{xc}(n_\uparrow, n_\downarrow)n(\mathbf{r}), \tag{2.12}$$

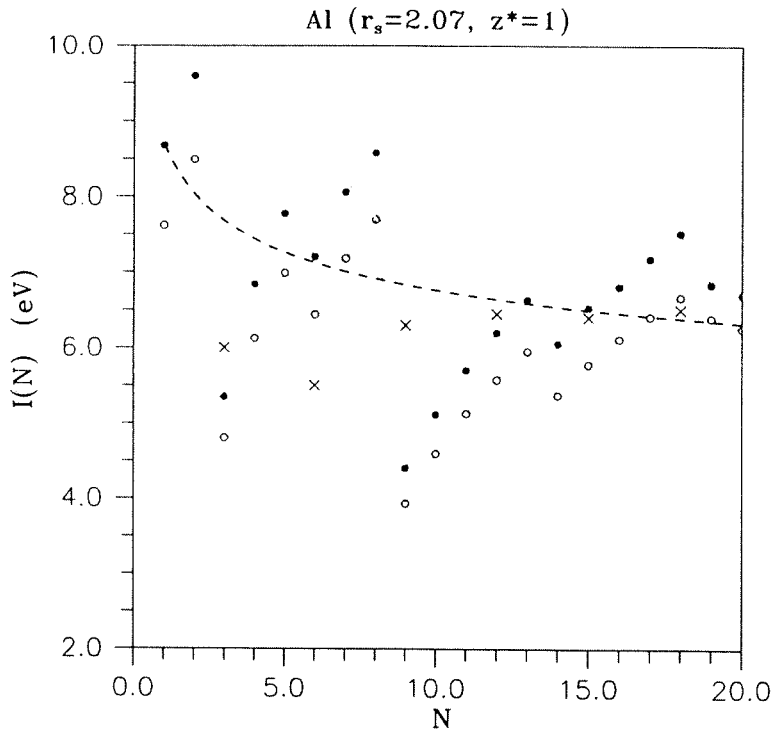

Figure 5. The same as Figure 2 for aluminum. Note that only N = 3, 6, 9, 12, 15, 18 are physically meaningful. Experimental data are taken from [23].

where

$$U[n] = \frac{1}{2}\int d^3r \int d^3r' \frac{n(\mathbf{r})n(\mathbf{r}')}{|\mathbf{r}-\mathbf{r}'|} \tag{2.13}$$

is the electronic Coulomb repulsion energy, and

$$U_B[n_+] = \frac{3}{5}\frac{N(N-N^{1/3})}{R} \tag{2.14}$$

is the background Coulomb repulsion minus the self-repulsion energy within each Wigner–Seitz cell. We have adopted the version of stabilized jellium in which the effective valence is unity ($z^* = 1$), since this version gives the more realistic bulk modulus. The ordinary jellium model is recovered by dropping the last term of Eqs. (2.7) ($r < R$) and (2.14).

For a spherical system, the self-consistent Eq. (2.5) is

$$-\frac{1}{2r^2}\frac{d}{dr}\left(r^2\frac{d\mathcal{R}_{\alpha\sigma}}{dr}\right) + \left(v_{\text{eff}}(\mathbf{r},\sigma) + \frac{l(l+1)}{2r^2} - \varepsilon_{\alpha\sigma}\right)\mathcal{R}_{\alpha\sigma} = 0\,, \tag{2.15}$$

where $\mathcal{R}_{\alpha\sigma} = \mathcal{R}_{nlm\sigma}$ is the radial wave function. As an approximation and to oblige the system to have spherical symmetry, we replace the true electronic spin density by the spherical average

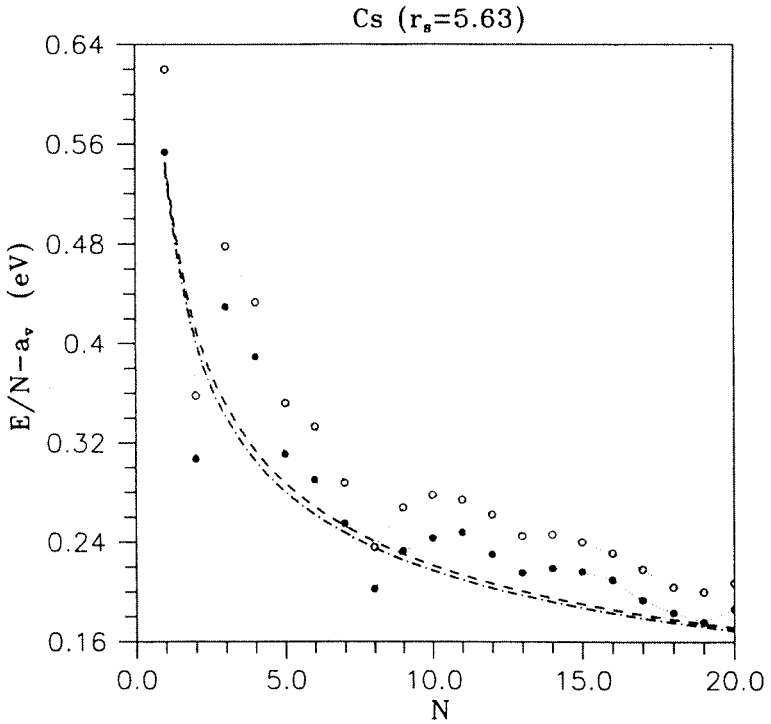

Figure 6. The same as Figure 1 for cesium ($r_s = 5.63$). The bulk binding energy is $a_v = -4.64$ eV for stabilized jellium and $a_v = -1.98$ eV for jellium.

$$n_\sigma(\mathbf{r}) = \frac{1}{4\pi} \sum_{nlm} |\mathcal{R}_{nlm\sigma}(\mathbf{r})|^2 . \tag{2.16}$$

In order to solve (2.15), with the approximation (2.16), we have used an atomic code where the nucleus with constant charge has been expanded to the desired cluster radius.

It is known that the energy of a finite quantal system, such as a cluster, can be described in an average way by the liquid drop model (LDM)

$$E_{\mathrm{LDM}}(N) = a_v N + a_s N^{2/3} + a_c N^{1/3} + \cdots \tag{2.17}$$

The coefficients a_v (volume), a_s (surface), and a_c (curvature) for the stabilized jellium model have been obtained with the aid of the so-called "leptodermous expansion" [8]. They are given in Table I for Al, Na, and Cs.

We can write (2.17) in the form

$$E_{\mathrm{LDM}}(N) = a_v N + a_s(N) N^{2/3}. \tag{2.18}$$

The Padé formula for a stable cluster is [6]

$$a_s(N) = a_s[1 - b_1 N^{-1/3} + b_2 N^{-2/3} - b_3 N^{-1}]^{-1} . \tag{2.19}$$

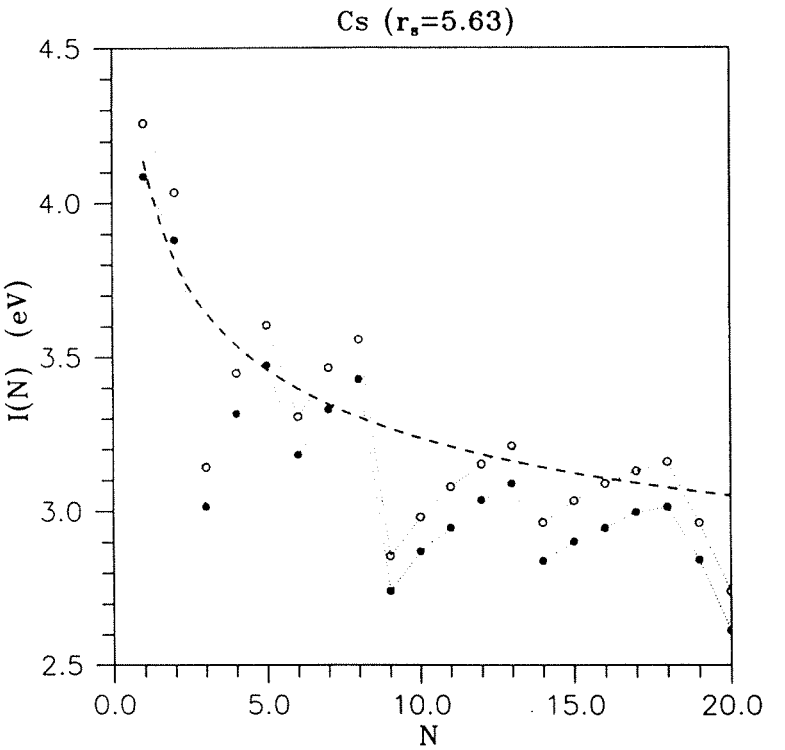

Figure 7. The same as Figure 2 for cesium.

The coefficients b_1, b_2, and b_3 are given in Table II. This formula was developed to connect the liquid drop expansion for a spherical void of large radius with the perturbation expansion for a void of small radius. It effectively sums the leptodermous expansion to all orders, and has been adapted to clusters by changing the sign of the curvature R^{-1}.

We compare the liquid drop prediction with the quantal result, looking for special stability (shell closures) for numbers N such that

$$E(N) < E_{\mathrm{LDM}}(N) . \tag{2.20}$$

Relative stability is also indicated by local maxima of the ionization energy

$$I(N) = E_N(N-1) - E_N(N) , \tag{2.21}$$

where the subscript N denotes the fixed positive charge. A smooth formula for the ionization energy is

$$I(N) = W + \frac{1}{2(r_s N^{1/3} + x_0)} , \tag{2.22}$$

with W the work function and x_0 the location of the image plane for the planar surface. (The values in Table I are taken from [9].) Eq. (2.22) is an approximation

TABLE III. Cohesive energies for the stabilized jellium (SJ) and jellium (J) models (in eV), using different approximations: "LSD" means local-spin-density, "LDA" local-density approximation, "SIC" self-interaction correction, "LDM" liquid drop model, "Padé" Padé approximant, and "Exp" experiment (from [18]). Here we use densities which are slightly different from those of Table I. The values in this table refer to zero temperature, while the previous ones are room temperature values.

	r_s (bohr)		LSD	LDA	SIC	LDM	Padé	Exp.
Al ($N = 3$)	2.07	SJ	3.79	3.93	3.21	2.75	3.02	3.34
		J	0.72	0.84	0.21	−0.25	−0.07	
Al ($N = 1$)	2.07	SJ	1.91	2.41	1.61	1.52	1.90	—
		J	0.48	0.91	0.24	0.08	0.19	
Na	3.93	SJ	0.92	1.18	0.81	0.85	0.82	1.13
		J	0.88	1.15	0.78	0.82	0.78	
Cs	5.62	SJ	0.56	0.74	0.51	0.59	0.54	0.83
		J	0.62	0.81	0.57	0.66	0.76	

to the liquid drop expression [10], in which a weakly size-dependent LDM chemical potential $\mu(R) \approx -W$ appears.

A third measure of stability is the second-order energy difference, which has been used to interpret mass spectra of metallic clusters:

$$\Delta_2(N) = E(N+1) + E(N-1) - 2E(N)\,. \tag{2.23}$$

A peak of this quantity means an enhancement of stability with respect to neighboring values of N. In the liquid drop model, Eq. (2.23) becomes $\Delta_2(N) = \partial^2 E_{\mathrm{LDM}}(N)/\partial N^2$. We shall see whether the criteria for relative stability based on (2.20), (2.21), and (2.23) agree.

Results

Bulk jellium is stable at the density $r_s = 4.2$, where $\langle \delta v \rangle_{\mathrm{WS}} = 0$. Sodium ($r_s = 3.99$) has therefore been used as an application of the jellium model [11,12]. Since the stabilized jellium model yields a small value of $\langle \delta v \rangle_{\mathrm{WS}}$ for Na, the surface properties of jellium and stabilized jellium should be practically the same for this metal, although the bulk binding energy per particle a_v is very different in the two models. Small clusters of Na are more bound in the stabilized jellium description than in jellium (see Fig. 1, noting the different a_v for stabilized jellium and jellium). Nevertheless, the shell structure, i.e., the oscillation around the smooth curve given by the liquid drop formula, is essentially the same, with magic numbers $N = 2$, 8, 18, 20. The binding energy is also well below the LDM curve for $N = 19$, where the $2s$ shell is half-filled. For the electron numbers $N = 1$, 7, 9, 17, the quantal result agrees closely with the LDM prediction. These "tell-tale" numbers might be used to estimate the exact (beyond LSD) surface and curvature energies from careful quantum-chemical calculations for small spherical clusters. For Na, the Padé representation practically coincides with the liquid drop formula.

The shell structures of jellium and stabilized jellium are also displayed by the ionization energies. The ionization energies of the two models agree closely (Fig. 2). The ionization energy for $N = 19$ is bigger than that for $N = 20$; this fact, known for jellium in LSD [13], holds for stabilized jellium as well. The local maxima at half-filled shells ($N = 5, 13$) are a characteristic of LSD, and are not seen in the local-density-approximation (LDA) [14]. (LDA is LSD with $n_\uparrow$, $n_\downarrow$ replaced by $n/2$, $n/2$.)

Figure 2 also presents experimental ionization energies for Na clusters. For the smallest clusters, the spherical stabilized jellium results are not in good agreement with experiment. In fact, clusters of five or fewer atoms are typically planar [15,16]. Moreover, the instability of many spherical open-shell clusters is evident from the total energies of Figure 1. For example, the total energy for $N = 3$ is greater than the sum of total energies for $N = 2$ and 1. These unstable clusters will start to deform away from spherical shape toward fission. In many cases, they will reach energy minima before fission occurs. Spheroidal distortions can correct most of the difference between our ionization energies and experimental ones [17].

The second-order energy difference is almost identical in jellium and stabilized jellium (Fig. 3). The liquid drop result for $\Delta_2(N)$ is practically constant ($\Delta_2(N) \approx 0$), providing a good average of the quantal values.

Turning to Al, we find that the shell fluctuations are bigger than for sodium, although the two patterns are similar (Fig. 4). The Padé approximant and the LDM formula agree, except for the smallest clusters ($N \leq 8$). For $N = 1$, the Padé formula reproduces the quantal energy; recall that N is the number of valence electrons and not the number of atoms. The ionization energies of stabilized jellium (Fig. 5) are bigger that those of jellium, although the peak structure is the same. For $N \geq 12$, our results agree with experiment.

In the case of Cs (Figs. 6 and 7), the nonbulk binding energies $E/N - a_v$ and the ionization energies of stabilized jellium are below those of jellium. As expected, a negative value of $\langle \delta v \rangle_{WS}$ (as in Al) increases the nonbulk binding energy $E/N - a_v$, the ionization energy, and the amplitude of $\Delta_2(N)$ oscillations, while a positive value (as in Cs) has the opposite effects.

The cohesive energy is the energy difference between the free atom and an atom in the bulk. It can be written as

$$\varepsilon_{coh} = -a_v z + E(N = z)\,, \tag{3.1}$$

where z is the valence of the atom. This quantity can be read directly from Figures 1, 4, and 6. Table III gives values for the cohesive energy of stabilized and ordinary jellium, in different approximations.

In the case of Al, an atom of stabilized jellium is a cluster with $\langle \delta v \rangle_{WS}$ constructed from an effective valence $z^* = 1$, but with $N = 3$ electrons (real valence). We have also included in Table III the case $N = 1$, since this provides a fair test of the LDM and Padé formulas.

We see from Table III that stabilization of jellium drastically improves the cohesive energy of Al, in comparison with experiment. Table III also shows that the Padé successfully predicts the LSD cohesive energies of monovalent metals ($N = 1$); the

discrepancy for $N = 3$ may be attributed to shell effects. Our LDA values agree with the "ideal metal" results of Rose and Shore [18]. The surface and cohesive properties of the ideal metal are the same as those of stabilized jellium; the small difference we find arises from the use of a different correlation energy. We note that the LDA cohesive energies are close to experimental ones. However, this close agreement is due to a cancellation of errors between the LDA and the stabilized jellium approximation. The *exact* cohesive energy for monovalent stabilized jellium is given by the self-interaction correction (SIC) [19], and is smaller than the LSD value.

Conclusions

We have analyzed the properties of small clusters of stabilized jellium. Stabilized jellium is similar to the pseudojellium model of Utreras-Díaz and Shore [20], but unlike the latter it does not use phenomenological information other than the density. Binding energies, ionization energies, second-order energy differences, and cohesive energies have been calculated. The shell structure is essentially the same for ordinary and stabilized jellium. The various measures of stability tend to agree. The cohesive energies are more realistic in the stabilized jellium model than in the ordinary one, particularly for Al.

Future work with stabilized jellium could investigate different breakup channels for charged clusters (a problem which has been studied within the ordinary jellium model [14]), self-compression effects (since a cluster should have a central density bigger than the bulk value [5]), large clusters (e.g., the analysis of supershells [21]), and the static and optical response of clusters.

Acknowledgments

The work of two of the authors (C.F. and J.P.) was supported by NATO collaborative research Grant 910623. That of one of the authors (J.P.) was supported by the U.S. National Science Foundation under Grant DMR92-13755. C.F. acknowledges a travel grant from the Calouste Gulbenkian Foundation, which made possible the presentation of this work at the 1993 Sanibel Meeting.

Bibliography

[1] J. P. Perdew, H. Q. Tran, and E. D. Smith, Phys. Rev. **B42**, 11627 (1990).
[2] W. de Heer, W. Knight, M. Chou, and M. Cohen, *Solid State Physics*, Vol. 40, H. Ehrenreich and O. Turnbull, Eds. (Academic, New York, 1987), p. 93.
[3] M. Brack, Rev. Mod. Phys. (1993), to appear in July.
[4] W. de Heer, Rev. Mod. Phys. (1993), to appear in July.
[5] J. P. Perdew, C. Fiolhais, and M. Brajczewska, unpublished.
[6] J. P. Perdew, P. Ziesche, and C. Fiolhais, Phys. Rev. **B47** (1993).
[7] S. H. Vosko, L. Wilk, and M. Nusair, Can. J. Phys. **58**, 1200 (1980).
[8] C. Fiolhais and J. P. Perdew, Phys. Rev. **B45**, 6207 (1992).
[9] A. Kiejna, Phys. Rev. **B47**, 7361 (1993).
[10] J. P. Perdew, in *Condensed Matter Theories*, Vol. 4, J. Keller, Ed. (Plenum, NY, 1989).
[11] D. R. Snider and R. S. Sorbello, Solid State Comm. **47**, 845 (1983).
[12] D. E. Beck, Solid State Comm. **49**, 381 (1984).

[13] P. Ballone, C. J. Umrigar, and P. Delaly, Phys. Rev. B**45**, 6293 (1992).
[14] Y. Ishii, S. Ohnishi, and S. Sugano, Phys. Rev. B**33**, 5271 (1986).
[15] U. Röthlisberger and W. Andreoni, J. Chem. Phys. **94**, 8129 (1991).
[16] R. O. Jones, Phys. Rev. Lett. **67**, 224 (1991).
[17] W. Ekardt and Z. Penzar, Phys. Rev. B**38**, 4273 (1988).
[18] J. H. Rose and H. B. Shore, Phys. Rev. B**43**, 11605 (1991).
[19] J. P. Perdew and A. Zunger, Phys. Rev. B**23**, 5048 (1981).
[20] C. A. Utreras-Díaz and H. B. Shore, Phys. Rev. B**40**, 10345 (1989).
[21] J. Meyer, unpublished.
[22] M. M. Kappes, M. Schär, U. Röthlisberger, Ch. Yeretzian, and E. Schumacher, Chem. Phys. Lett. **143**, 251 (1988).
[23] M. F. Jarrold, J. E. Bower, and J. S. Kraus, J. Chem. Phys. **86**, 3876 (1987).

Received April 29, 1993